MODELING MICROMILLING CUTTING FORCE ON MACHINING ALUMINUM ALLOY

Fábio Oliveira Campos, Adriane Lopes Mougo, Anna Carla Araujo

22nd International Congress of Mechanical Engineering (COBEM 2013)
November 3-7, 2013, Ribeirão Preto, SP, Brazil

MODELING MICROMILLING CUTTING FORCE ON MACHINING ALUMINUM ALLOY

Fábio de Oliveira Campos
Adriane Lopes Mougo
Anna Carla Araujo
CEFCON - Machining Research Laboratory
Mechanical Engineering Department, COPPE/UFRJ, Rio de Janeiro, Brazil
fabiocampos23@bol.com.br
adriane.mougo@gmail.com
anna@mecanica.ufrj.br

Abstract. *Micro end milling is one of the manufacturing processes that produces micro topography using mechanical removal of chips. Its modeling presents some peculiarities compared to meso scale process. This article presents a mechanistic model for micromilling process considering homogeneous grain properties. It is not taken into account dynamic behavior of tool and interaction between tool-workpiece due to stiffness or grain variation. The model uses calibration method based on experimental data used to calculate specific pressure. The design of experiments considers feed rate and cutting velocity as factors and resultant force as the output. The model is validated using experiments inside the DOE factors range. The result presents the comparison between calculated and experimental values for the cutting force and the maximum error presented 8% of difference.*

Keywords: *Micromilling; Metal Cutting Force; Mechanistic models*

1. INTRODUCTION

Miniaturization has increased over the last decade and, as a consequence, manufacturing of micro parts for bioengineering and aerospace applications are one of the areas where there is a need of research and development. Micromilling is a flexible machining process that allows the fabrication of high quality parts. Cutting force analysis plays a vital role in studying the micromilling processes. The stress variation on the shaft of a microtool is much higher than that on a conventional tool. As the feed per tooth in micrommilling operations to tool radius ratio has to be higher than in conventional milling to keep productivity at a reasonable level (Bao and Tansel, 2000). Due to the small size of the microtools, it is very difficult to notice the damage in the cutting edges and an inappropriate selection of the cutting conditions can cause the tool to brake unexpectedly. The microtools used in this operation have a diameter of less than 2 mm.

In machining of metallic components, the size of the part plays an important role, called size effect. Even if the relationship between the main geometrical features is kept constant, the process behavior changes. Vollertsen *et al.* (2009) presented a review on effects of size effect and their use: the article presents the typology of size effect, a description of size effect on strength and tribology and size effects on formability and machinability. Câmara *et al.* (2012) presented a state of art on micromilling with emphasis on the work material requirements, tool materials and geometry, cutting forces and temperature, quality of the finished product, burr formation, process modeling and monitoring and machine tool requirements.

Two process mechanisms, ploughing and chip formation, are involved in micromachining. A critical cutting thickness needs to be exceeded to involve both phenomena. Ramos *et al.* (2012) studied the minimum uncut chip thickness. Besides the ploughing mechanism, where part of the material is plastically pushed against the workpiece surface when $t_c < t_{c_{min}}$, there is also the mechanism of elastic deformation, when the deformation forces are proportional to the interference volume between the tool and the workpiece when $t_c << t_{c_{min}}$ (Vogler *et al.*, 2004). Malekian *et al.* (2012) used the minimum uncut chip thickness, under which the material is not removed but ploughed, and claimed that this effect causes an increase of machining forces that affect the surface integrity of the workpiece.

Microstructure has a significant effect on microscale cutting. Simoneau *et al.* (2007) investigates the effect of grain size and orientation during microcutting in FE modeling of the primary shear zone. Their research group (Simoneau *et al.*, 2006) analyzed the orthogonal cutting in microscale. Tests were conducted on steel and the resulting chips examined, showing that the chip formation changes from continuous to "quasi-shear-extrusion" chip due to the uncut thickness size. The results indicate that the pearlite and softer ferrite grains play distinct roles in the plastic deformation process. Abouridouane *et al.* (2012a) investigate size effect by down scaling the twist drilling using a Lagrangian formulation proposed in the implicit code. He also presented a new three-dimensional multiphase finite element computation model for the simulation of micro drilling two-phase ferritic-pearlitic carbon steels (Abouridouane *et al.*, 2012b). This article analysed the cutting mechanism, the ploughing phenomena, tribological and heat transfer mechanisms at the microscale. Jin and Altintas (2012) presents the prediction of micromilling forces using cutting force coefficients evaluated from the

finite element simulations of orthogonal microcutting process and compared to experimental turning results. The milling forces in their model are calculated based on the local geometry and chip load.

Bao and Tansel (2000) proposed an analytical force model for micro end milling process based on Tlusty's model (Tlusty and MacNeil, 1975), but using a new expression for the chip thickness. They computed by the trajectory of the tool tip and observed that the model gives a good result at higher feed rate which supports his assumption that feed per tooth to tool radius is larger in micro end milling than in the conventional end milling operation. Zaman *et al.* (2006) established a new concept to estimate the cutting force in micro end milling by estimating the theoretical chip area instead of undeformed chip thickness. Pérez *et al.* (2007) developed a new model for the estimation of cutting forces in micromilling based on specific cutting pressure. The proposed model includes three parameters which allow to control the entry of the cutter in the workpiece and which consider also the errors in the radial position of the cutting edges of the tool. The new mechanistic force model determines the instantaneous cutting force coefficients using experimental data processed for one cutter revolution. The model has been validated through experimental tests over a wide range of cutting conditions. The results obtained show good agreement between the predicted and measured cutting forces. Rodríguez and Labarga (2013) developed a new cutting force prediction model in micromilling operations for application on machining monitoring systems, considering the most influents factors of the process, like tool deflection, runout, scale effect and. Experiments carried out on Aluminum 7075 and AISI 1045 steel presented a good concordance with simulated results. Kang *et al.* (2007) developed a mechanistic model to predict the cutting force in micro milling and its influence on tool wear and superficial roughness of Al 7075 alloy. Experimental results showed good concordance and the raise of the feed per tooth indicated a raise of the cutting force values.

This article uses experimental data of cutting force to calibrate and validate a model for estimation of the specific pressure. Also, a mechanistic cutting force model is compared with the cutting force data, considerig homogeneous grain properties of the material. It was not considerated any dynamic behavior of the tool, like the tool run-out, tool and machine vibrations or deflection of the tool.

2. CUTTING FORCE MODELING

The knowledge of cutting forces is fundamental for tool optimization and it is very important to avoid tool breakage and instability. In micro milling, those factors are even more relevant due to the high cost of tools, which break very easily. The conventional model for prediction of cutting forces based on the load that the tool makes on the chip is widely applied in mesoscale milling. However, to use it in micromilling, it is necessary to make few adaptations. In this work, we consider the main differences between macro and micromilling which are the difference in the uncut chip thickness and the appearance of the ploughing mechanism due to the scale effect.

2.1 Chip load cutting model

Elemental normal and frictional forces are required to the determination of cutting forces for a given geometry. The mechanistic modeling approach is a combination of analytical and empirical methods in which the forces are proportional to the chip load (Kline *et al.*, 1982). The specific cutting pressure, K_n, K_f and K_z, have been shown as a function of chip thickness t_c in mesoscale milling process and it is used for calculation of dF_n, dF_f and dF_z on each angular position θ of the discretized cutting edge proportional to the chip load area dA as shown in Eq. 1.

$$\begin{aligned} dF_t(\theta) &= K_t dA(\theta) \\ dF_r(\theta) &= m_1 K_t dA(\theta) \\ dF_z(\theta) &= m_2 K_t dA(\theta) \end{aligned} \tag{1}$$

Using a semi empirical modeling as Tlusty and MacNeil (1975), relating specific cutting pressures by empiric factors m_1 and m_2. Chip area is calculated based on uncut chip thickness $t_c(\theta)$, which is called Martellotti equation:

$$t_c(\theta) = f_t sin(\theta) \tag{2}$$

The mechanistic models consider that the specific cutting pressure is calculated in the form:

$$\ln K_t = a_0 + a_1 \ln t_c + a_2 \ln V_c + a_3 \ln (t_c.V_c) \tag{3}$$

where a_0, a_1, a_2 and a_3 are called specific cutting energy coefficients. They are dependent on the tool and workpiece

materials and also on the cutting speed and the chip thickness. They are determined from calibration tests for a given tool-workpiece combination and for a given range of cutting conditions.

2.2 Chip thickness correction in microcutting

Bao and Tansel (2000) developed a more precise expression than Martelotti calculation for uncut chip thickness $t_c(\theta)$ used by Newby *et al.* (2007) to calculate average uncut thickness.

$$t_c(\theta) = f_t sin(\theta) - \frac{z}{2\pi r} f_t^2 sin(\theta) cos(\theta) + \frac{f_t^2}{2f} cos^2(\theta) \tag{4}$$

Ploughing effect occur under minimum uncut chip thickness, which was modeled by different approaches. Liu *et al.* (2006) modeled considering analytical model using slip line theory and Johnson-Cook model. Malekian *et al.* (2012) presented an article on micromilling of aluminium, which is used in this article based on the edge radius r_e and on a critical or stagnant angle, φ_m, equal to the friction angle between the material and the rake face, regardless of the other parameters involved in the process.

$$t_{cm} = r_e(1 - cos(\varphi_m)) \tag{5}$$

3. EXPERIMENTAL SETUP

In order to analyze the cutting forces involved in the process of micromilling and compare them to the forces predicted by the models presented before, a series of experiments were performed.

3.1 Material, tools and experiments

The material selected for the experiments was an aluminum alloy (Al 6351-T6), which is an AlMgSi alloy usually applied in the automotive, construction engineering and shipbuilding industries. The overall workpiece dimensions were 47x50x15 mm, in which a small area were faced to be subjected to the experimental machining. It was used a carbide micromilling tool, very often applied in medical, aerospace and electronic areas, with 0.381 mm diameter and 1.143 mm flute length, as showed in Fig. 1 (**?**) based on manufacturer information.

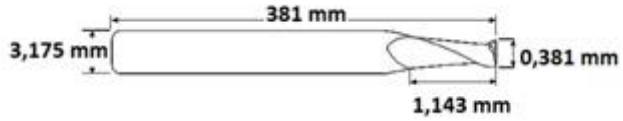

Figure 1: Dimensions of the micromilling tool used on the experiments

As the cutting edge radius has strong influence on the cutting force model chosen, it is necessary to analyze the microtool geometry. The cutting tool was measured in a scanning electron microscopy (SME). The images presented on Fig. 2 were taken. Using those SEM images, the helix angle, point radius and cutting edge radius were measured. The tool has point tip radius of 2,5 μm, cutting edge radius of 0,5 μm and $\beta = 30^\circ$ helix angle.

The micro machine-tool used on the experiments was the CNC Mini Mill/GX from Minitech Machinery Corporation. The machine uses NSK 60k RPM precision spindle with 3 axis controller. Its standard resolution is 0.78125 μm using dual linear ball bearing slides on each axis, sealed for the table mechanism (THK linear slides - RSR15 series, caged-ball technology). The drive mechanism THK Ball Screw actuator - preloaded and sealed, achieves low torque fluctuation and no backlash.

A minidynamometer was used for cutting force measurement: the MiniDyn 9256C2 from KISTLER with cable 1697A5, as shown in Fig. 3a. The cutting force components are presented in the Fig. 3a. It was used a KISTLER charge amplifier 5070A10100 and a data acquisition board USB 6251 from National Instruments. The minidynamometer was calibrated with a sensitivity of -25.61 pC/N on F_x, -12.86 pC/N on F_y and -25.86 pC/N on F_z. The frequency of data acquisition was 40000Hz and a amplifying rate of 2 N/V was used on the charge amplifier. Table 1 summarizes the equipment used on the setup.

3.2 Experimental Procedure

Before the actual micromilling experiments started, a surface of 50 x 20 mm, the work area, was faced on the workpiece using a 3mm milling tool, as shown in the Fig. 3b. It was used 18 m/min as cutting velocity and feed rate equals to 200 mm/min. This facing operation is important because it ensures that the micromilling operation would be performed on a

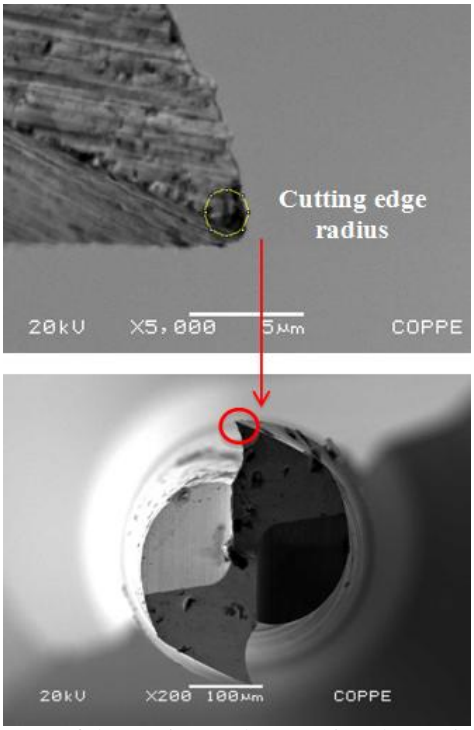

Figure 2: SEM images of the cutting tool presenting the cutting edge radius (r_e)

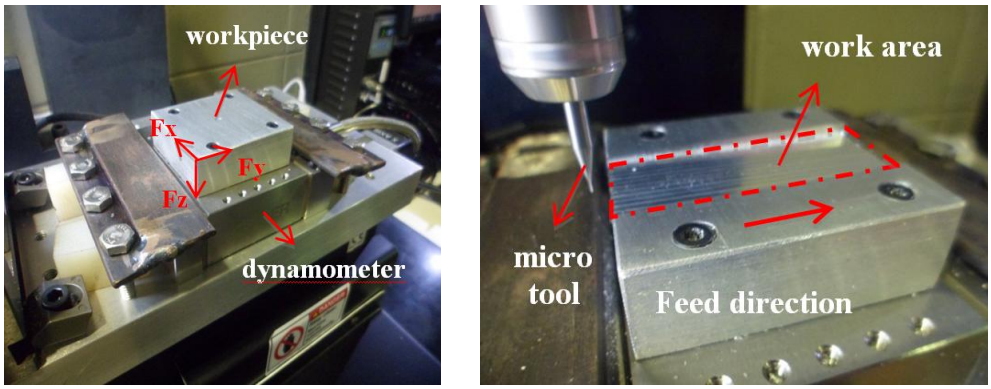

(a) MinyDyn and force components (b) Feed direction and work area

Figure 3: Experimental setup

Table 1: Equipment specifications

Equipment	**Specifiction**
Micromilling Machine	Minitech Machinery CNC Mini-Mill GX
Charge Amplifier	Kistler 5070A10100
Oscilloscope	National Instruments USB 6251
Dynamometer	Kystler Mini Dyn 9256C2
SEM	ZEISS DSM 940

flat surface. If the surface to be machined wasn't flat, the axial depth of cut could vary during the cutting process and, consequently, the forces data would not be right.

The micromilling tool performed a surface trajectory before each pass to guarantee the axial depth of cut designed. The axial depth of cut chosen is more than 20 times higher then the point radius, 100 μm. That is why the main cutting edge has more significance impact on the cutting model. The secondary cutting edge was neglected.

The experiments were planned to analyze the influence of two factors, with three levels each, on the cutting force. The factors chosen were the feed per tooth and the cutting velocity. Considering the cutting edge radius of 0,5 μm, three feed per tooth (f_t) values from 1 to 5 μm were planned for running tests. These values are almost 10 times higher then the radius measured before. This choice was made in order to use cutting models that does not considers ploughing as the

main component of the cutting force. Also, it was chosen three different cutting velocities: 20000, 25000 and 30000 rpm. Two replicates were performed for the first spindle speed level and three replicates for the other parameters combination. It was used clockwise spindle apeed and no cutting fluid. Table 2 presents the cutting parameters used on the experiments.

Table 2: Cutting parameters

Cutting Velocity	23.93, 29.9 and 35.89 m/min
Feed per tooth	2, 4 and 5 μm/tooth
Axial Depth of Cut	100 μm
Width of Cut	381 μm (full immersion)
Length of Cut	15 mm
Workpiece Material	Al 6351 T6

The first and third levels of each parameters would be used to calibrate the calculation of the specific cutting pressure. And the second level will validate, or not, the calculation. Summarizing the design of the experiments, the order of the replicates as well as the cutting parameters used in each replicate are shown in Tab. 3. The order of the experiments was planned in a way to ensure the randomization of them.

Table 3: Design of Experiments

Tests	**Experiment**	**Replicate**	**Feed per Tooth (mm/th)**	**Spindle Speed (rpm)**
1	1	1	0.002	20000
2	2	1	0.005	20000
3	1	2	0.002	20000
4	2	2	0.005	20000
5	5	1	0.004	20000
6	5	2	0.004	20000
7	3	1	0.002	30000
8	4	1	0.005	30000
9	4	2	0.005	30000
10	6	1	0.004	25000
11	3	2	0.002	30000
12	6	2	0.004	25000
13	6	3	0.004	25000
14	3	3	0.002	30000
15	4	3	0.005	30000

4. RESULTS AND DISCUSSION

In this section it is presented the experimental data, the simulated curves and the calculation of basic specific cutting pressure.

4.1 Experimental results

Figure 4 shows the cutting force signals in X and Y direction for a replicate of each experiment. The signals were filtered using a high-pass filter with the cut-off frequency corrsponding to the frequency of the spindle speed, as it was noticed that even when the tool is not cutting, but with the feed and the spindle on, there is a high noise level in the force component in the feed direction. The force components presented (F_x and F_y) represents the components on the plane normal to the spindle, as presented on Fig. 3a.

Analyzing the graphs of the experimental cutting force showed on Fig. 4, it can be verified that the run-out of the tool is small when milling with 2000 rpm as spindle speed, as the difference between the peaks of the two flutes is very small. However, when the speed used is greater, it can be noticed the difference between the force peaks for each flute of the tool, evidencing the raise of the run-out.

To analyze the signal, the cutting data of twenty revolutions of the tool was chosen and the maximum resultant force of each revolution was selected. An average of these maximum forces was calculated so the resultant cutting pressure can be computed.

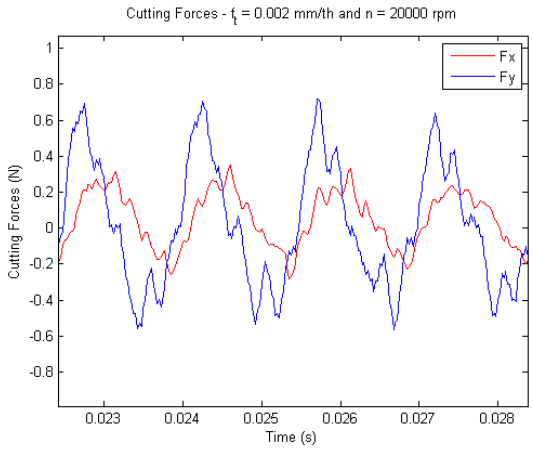

(a) Experiment 1

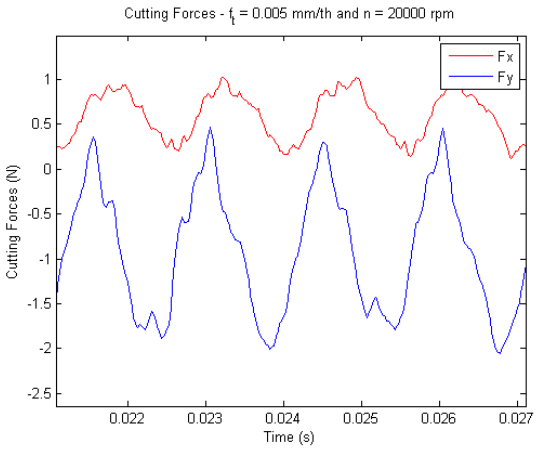

(b) Experiment 2

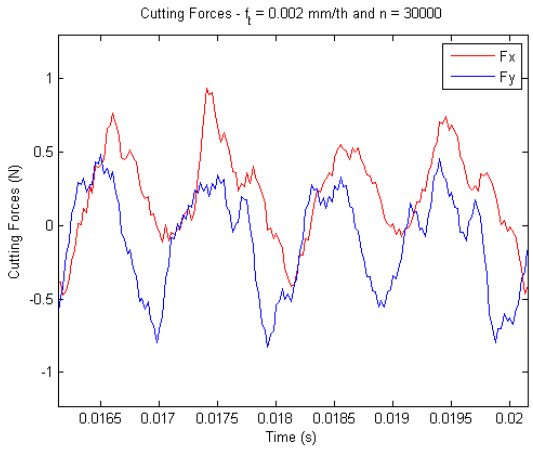

(c) Experiment 3

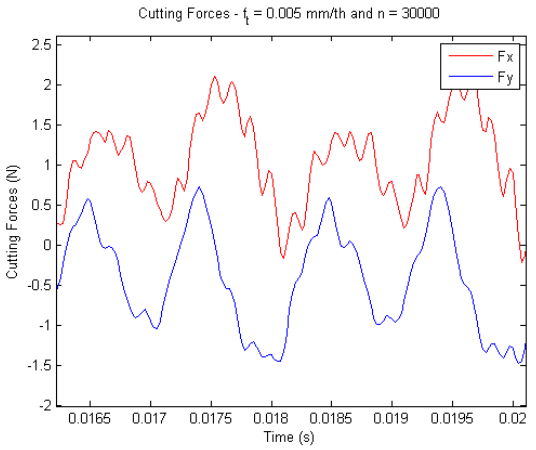

(d) Experiment 4

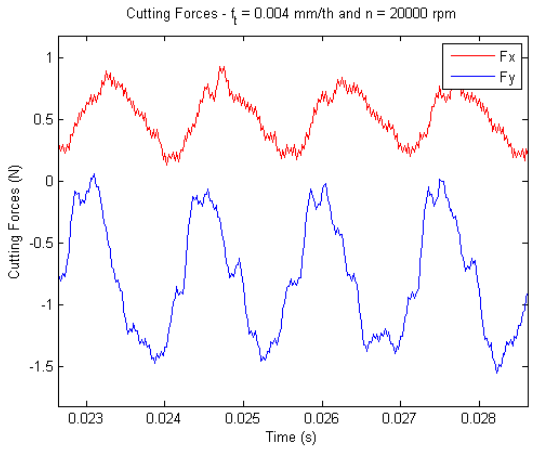

(e) Experiment 5

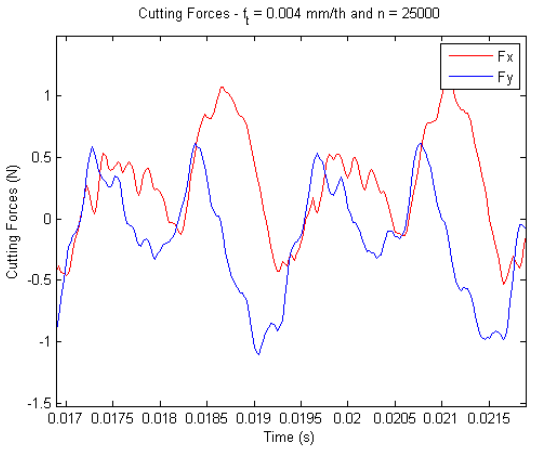

(f) Experiment 6

Figure 4: Experimental cutting forces for a replicate of each experiment

4.2 Specific cutting force

Using the experimental results of Malekian *et al.* (2009), m_1 and m_2 on Eq. 1 are 0.6 and 0.2, respectiveley. Using average maximum force and the maximum chip area - feed times depth of cut - was used and the resultant cutting pressure can be calculated. Then, the experimental specific cutting pressure for each experiment is given by:

$$K_t = \frac{K_{res-max}}{\sqrt{1 + 0.6^2 + 0.2^2}} \tag{6}$$

Using Eq. 3 and computing the experimental specific cutting pressure, the coefficients a_0, a_1, a_2 and a_3 can be calculated by solving a linear system. Then the numerical specific cutting pressure can be calculated and compared with the experimental. The experiments number 1, 2, 3 and 4 are used to calibrate the model and the experiments 5 and 6 to validate it. After solving the linear system, Eq. 3 becomes:

$$\ln K_t = 5.3019 - 0.2857 \ln t_c + 0.5456 \ln V_c + 0.2599 \ln (t_c.V_c) \tag{7}$$

Figure 5 presents the effect of chip thickness and cutting velocity on the specific cutting pressure. It can be seen that the cutting velocity has double the effect that the chip thickness has on the specific cutting pressure.

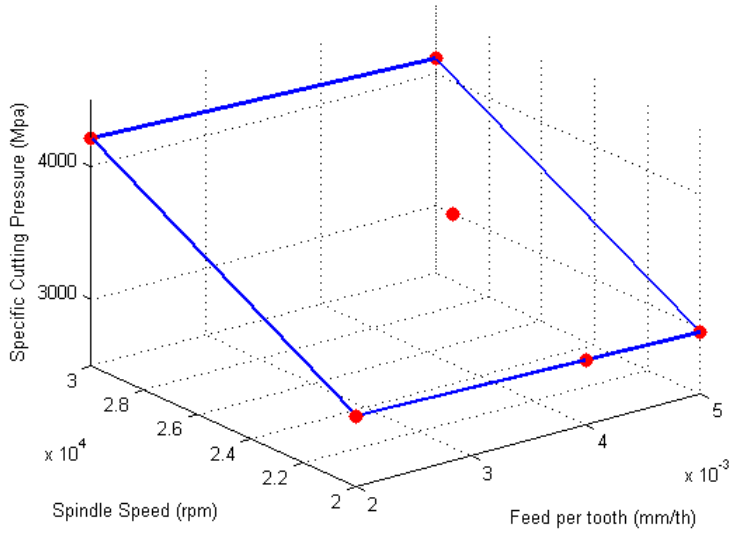

Figure 5: Effect of chip thickness and cutting velocity on specific cutting pressure

The error between the experimental specific cutting pressure and the numerical specific cutting pressure is shown in Tab. 4. Although it is not a very high error, the main reason why the error is not smaller is because the principal matrix of the linear system was ill-conditioned, that is, almost singular.

Table 4: Comparison between experimental and numerical specific cutting pressure

Experiment	**Experimental (Mpa)**	**Numerical (Mpa)**	**Error (%)**
K_{t_1}	2789.9	3038.9	8.93
K_{t_2}	3235.7	2966.4	-8.32
K_{t_3}	4593.3	4215.0	-8.24
K_{t_4}	3777.4	4116.5	8.98
K_{t_5}	2910.8	2990.6	2.74
K_{t_6}	3477.6	3627.0	4.29

4.3 Tool Wear

After the experiments, the tool was analyzed in SEM to verify the wear of it. It was noticed that the cutting point of both thoot was broken, as shown the comparison between the tool with no use and after the procedures in Fig. 6. In the figure, it is shown the size of the breakage. Considering the depth of 57.5 μm, at some of the experiment the tool probably started not to cut with the specified depth of 100 μm.

It is important to reaffirm that the specific cutting pressure computed before considers the original depth of cut. As we can not be sure of when the point of the tool broke, it was considered the worst case: with 100μm of depth of cut, the cutting force would be greater than with a smaller one. The results of the specific pressure are for the case where the cutting depth is bigger.

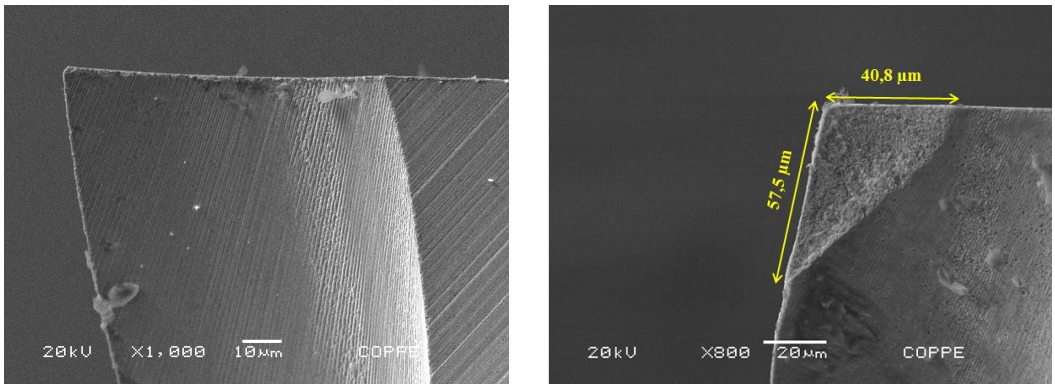

(a) New tool (b) Tool with wear

Figure 6: Comparison between the tool with no use and after the experiments

4.4 Simulation results

For comparison purposes, simulations were performed for the experiments 5 and 6 (Fig. 5) and they were used to calibrate the specifc cutting pressure model. It was used the experimantal values for the specific cutting pressure. The simulated cuting forces are presented in Fig. 7. It can be noticed that the profile of the forces are very similar to the experimental forces, but the values are much higher. This can be due to the tool wear verified after the experiments.

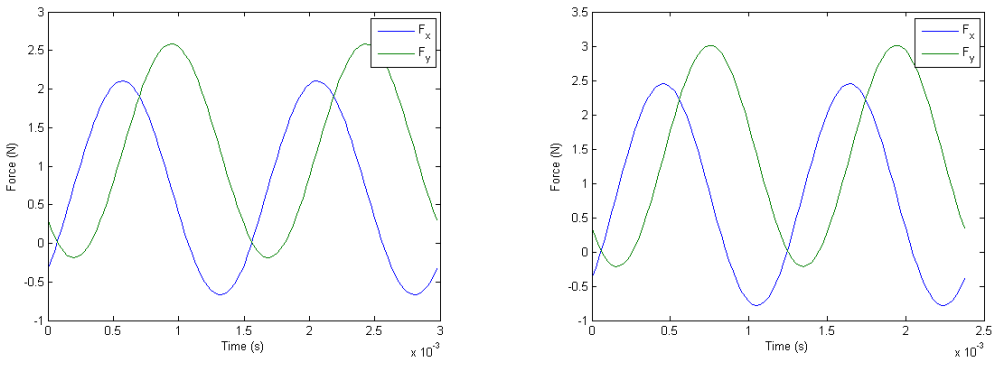

(a) Experiment 5 (b) Experiment 6

Figure 7: Simulated cutting forces for the parameters of the experiments 5 and 6

5. CONCLUSIONS

This article deals with micromilling of an aluminum alloy using three levels of feed rate and three levels of spindle speed, constant axial depth of cut and same tool. A semi-empiric model for calculation of cutting forces was used to calculate the specific cutting pressure.

The model was calibrated and validated with maximum error around 8%. It was confirmed, as expected, that the specific cutting pressure remains constant when varyng the spindle speed and increases with chip thickness. The experimental forces were compared to the forces simulated using a model for cutting force prediction om micromilling. The profile of the forces were similar, but the values of the simulated forces were higher. This difference can be related to the wear verified on the tool after the experiments. Some improvements must be made in the experimental procedure and relative to noise in the signal.

6. ACKNOWLEDGEMENTS

The authors thanks to the support of the CAPES for acquiring the equipment used in this article thru Pro-equipamentos resources, to the kindly services of UFRJ importation department, for the Mechanical Engineering Department for the

academic support and for PR-3 UFRJ to the support on conference expenses.

7. REFERENCES

Abouridouane, M., Klocke, F., Lung, D. and Adams, O., 2012a. "Size effects in micro drilling ferritic-pearlitic carbon steels". *Procedia {CIRP}*, Vol. 3, No. 0, pp. 91 – 96.

Abouridouane, M., Klocke, F., Lung, D. and Adams, O., 2012b. "A new 3d multiphase {FE} model for micro cutting ferritic–pearlitic carbon steels". *{CIRP} Annals - Manufacturing Technology*, Vol. 61, No. 1, pp. 71 – 74.

Bao, W. and Tansel, I., 2000. "Modeling micro-end-milling operations. part i: analytical cutting force model". *International Journal of Machine Tools and Manufacture*, Vol. 40, No. 15, pp. 2155 – 2173.

Câmara, M., Rubio, J.C., Abrão, A. and Davim, J., 2012. "State of the art on micromilling of materials, a review". *Journal of Materials Science & Technology*, Vol. 28, No. 8, pp. 673 – 685.

Jin, X. and Altintas, Y., 2012. "Prediction of micro-milling forces with finite element method". *Journal of Materials Processing Technology*, Vol. 212, No. 3, pp. 542 – 552.

Kang, I., Kim, J., Kim, J., Kang, M. and Seo, Y., 2007. "A mechanistic model of cutting force in the micro end milling process". *Journal of Materials Processing Technology*, Vol. 187–188, No. 0, pp. 250 – 255.

Kline, W., DeVor, R. and Lindberg, J., 1982. "The prediction of cutting forces in end milling with application to cornering cuts". *International Journal of Machine Tool Design and Research*, Vol. 22, No. 1, pp. 7 – 22.

Liu, X., Devor, R.E. and Kapoor, G., 2006. "An analytical model for the prediction of minimum chip thickness in micromachining". *Trans. ASME*, Vol. 128, pp. 474 – 481.

Malekian, M., Mostofa, M., Park, S. and Jun, M., 2012. "Modeling of minimum uncut chip thickness in micro machining of aluminum". *Journal of Materials Processing Technology*, Vol. 212, No. 3, pp. 553 – 559.

Malekian, M., Park, S.S. and Jun, M.B., 2009. "Modeling of dynamic micro-milling cutting forces". *International Journal of Machine Tools and Manufacture*, Vol. 49, No. 7–8, pp. 586 – 598.

Newby, G., Venkatachalam, S. and Liang, S., 2007. "Empirical analysis of cutting force constants in micro-end-milling operations". *Journal of Materials Processing Technology*, Vol. 192–193, No. 0, pp. 41 – 47.

Pérez, H., Vizán, A., Hernandez, J. and Guzmán, M., 2007. "Estimation of cutting forces in micromilling through the determination of specific cutting pressures". *Journal of Materials Processing Technology*, Vol. 190, No. 1–3, pp. 18 – 22.

Ramos, A.C., Autenrieth, H., Strauß, T., Deuchert, M., Hoffmeister, J. and Schulze, V., 2012. "Characterization of the transition from ploughing to cutting in micro machining and evaluation of the minimum thickness of cut". *Journal of Materials Processing Technology*, Vol. 212, No. 3, pp. 594 – 600.

Rodríguez, P. and Labarga, J., 2013. "A new model for the prediction of cutting forces in micro-end-milling operations". *Journal of Materials Processing Technology*, Vol. 213, No. 2, pp. 261 – 268.

Simoneau, A., Ng, E. and Elbestawi, M., 2006. "Chip formation during microscale cutting of a medium carbon steel". *International Journal of Machine Tools and Manufacture*, Vol. 46, No. 5, pp. 467 – 481.

Simoneau, A., Ng, E. and Elbestawi, M., 2007. "Grain size and orientation effects when microcutting {AISI} 1045 steel". *{CIRP} Annals - Manufacturing Technology*, Vol. 56, No. 1, pp. 57 – 60.

Tlusty, J. and MacNeil, P., 1975. "Dynamics of cutting in end milling". *Annals of CIRP*, Vol. 24, pp. 213 – 221.

Vogler, M.P., Kapoor, S.G. and DeVor, R.E., 2004. "On the modeling and analysis of machining performance in micro-endmilling, part ii: Cutting force prediction". *Journal of Manufacturing Sxience and Engineering*, Vol. 126, pp. 695 – 705.

Vollertsen, F., Biermann, D., Hansen, H., Jawahir, I. and Kuzman, K., 2009. "Size effects in manufacturing of metallic components". *{CIRP} Annals - Manufacturing Technology*, Vol. 58, No. 2, pp. 566 – 587.

Zaman, M., Kumar, A.S., Rahman, M. and Sreeram, S., 2006. "A three-dimensional analytical cutting force model for micro end milling operation". *International Journal of Machine Tools and Manufacture*, Vol. 46, No. 3–4, pp. 353 – 366.

8. RESPONSIBILITY NOTICE

The authors are the only responsible for the printed material included in this paper.